CRYSTAL GROWTH & DESIGN

Article

pubs.acs.org/crystal

Stress-Induced Crystallization of Ge-Doped Sb Phase-Change Thin Films

Gert Eising,* Andrew Pauza, and Bart J. Kooi*

Zernike Institute for Advanced Materials, University of Groningen, Nijenborgh 4, 9747AG Groningen, The Netherlands

ABSTRACT: The large effects of moderate stresses on the crystal growth rate in Ge-doped Sb phase-change thin films are demonstrated using direct optical imaging. For Ge_6Sb_{94} and Ge_7Sb_{93} phase-change films, a large increase in crystallization temperature is found when using a polycarbonate substrate instead of a glass substrate. This increase is attributed to the tensile thermal stress induced in the phase-change film due to a difference in thermal expansion coefficient between the film and the polycarbonate substrate. By applying a uniaxial compressive stress to a phase-change film, we show and explain that isotropic crystal growth becomes unidirectional (perpendicular to the uniaxial stress) with a strongly enhanced growth rate. This is a direct proof that modest stresses can have large consequences for the amorphous phase stability and for the crystal growth rates, and these stresses are thus highly relevant for memories based on phase-change materials.

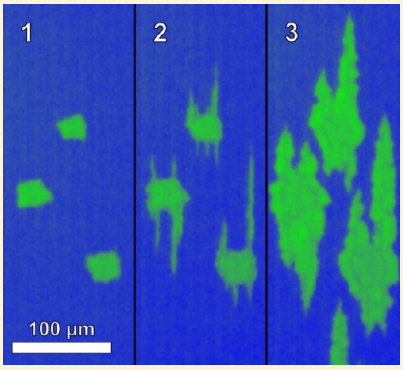

INTRODUCTION

Phase-change materials (PCMs) have aroused strong interest due to their suitability for electrical nonvolatile memory devices.[1−4] The ability to switch in tens of nanoseconds between the amorphous and crystalline phases at elevated temperatures used for switching while still having a long retention at the basic operating temperatures (e.g., <100 °C) in combination with the excellent prospects for downscaling makes PCM devices promising for next-generation memory devices and as a replacement for flash memory.[4] The stability and electrical resistance of the PCM cells are affected by stresses present in the cell,[5,6] and it is, therefore, of great importance to understand how these stresses influence the stability of the amorphous phase and the (re)crystallization process. Here, we show for the first time direct proofs that modest compressive stresses (e.g., 70 MPa) applied to PCM thin films can accelerate the crystal growth rate at a given temperature by a factor of 60. These results are highly relevant for memory devices because such modest stresses are easily introduced in the PCM in the devices and may even vary with this magnitude on a single bit level.

The switching of a PCM from amorphous to crystalline is, depending on the PCM composition, accompanied by a decrease in volume of typically 5−10%.[7] When the PCM has no degrees of freedom to expand or contract (for instance, in a memory cell) and the volume change is accommodated fully elastically, this would result in a (hydrostatic) stress on the order of GPa's. Most studied PCMs are, however, present in thin film form with a free surface, and then there is little constraint toward a dimensional change perpendicular to the surface. Only in-plane stresses on the order of a GPa can be expected. However, generally much smaller in-plane stresses are found, indicating that only a relatively small fraction of the volume change is accommodated elastically. The missing stress is thus relaxed by plastic deformation or viscous flow in the amorphous phase. For instance, approximately 9% of the total volume decrease upon crystallization (of various SbTe alloys with a film thickness of around 50 nm) was found to be transformed into elastic in-plane stress.[8] Nevertheless, this still leads to significant in-plane stresses of 100−200 MPa.

The decrease in volume upon crystallization suggests that a compressive stress aids the crystallization process. Indeed, under hydrostatic pressure, an amorphous $Ge_2Sb_2Te_5$ film was even crystallized at room temperature.[9] However, it was also found that, when capping layers exert an in-plane compressive stress on a thin $Ge_2Sb_2Te_5$ film, the crystallization temperature was increased.[10] However, the effect of capping layers on the stress state in the PCM was not determined in these cases, only showing the direct effect that capping layers can increase the crystallization temperature, particularly for extremely thin PCM films with a thickness below 10 nm. In contrast, there is clearly more convincing evidence that, upon crystallization, always tensile stresses develop in $Ge_2Sb_2Te_5$ films and that capping layers strongly increase the magnitude of the tensile stress.[11,12] Microcantilevers were used to act as sensors for measuring crystallization-induced density changes and stresses.[12] Still, these measurements only determine the response of the material system, but do not apply and systematically vary stresses to measure their influence on PCM properties. Here, we show for the first time the influence of applied stresses on the crystal growth in PCM films by employing a four-point bending stage and direct optical detection of the effect of applied compressive stresses.

Received: September 21, 2012
Revised: November 16, 2012
Published: December 5, 2012

   dx.doi.org/10.1021/cg3013848 | *Cryst. Growth Des.* 2013, 13, 220−225

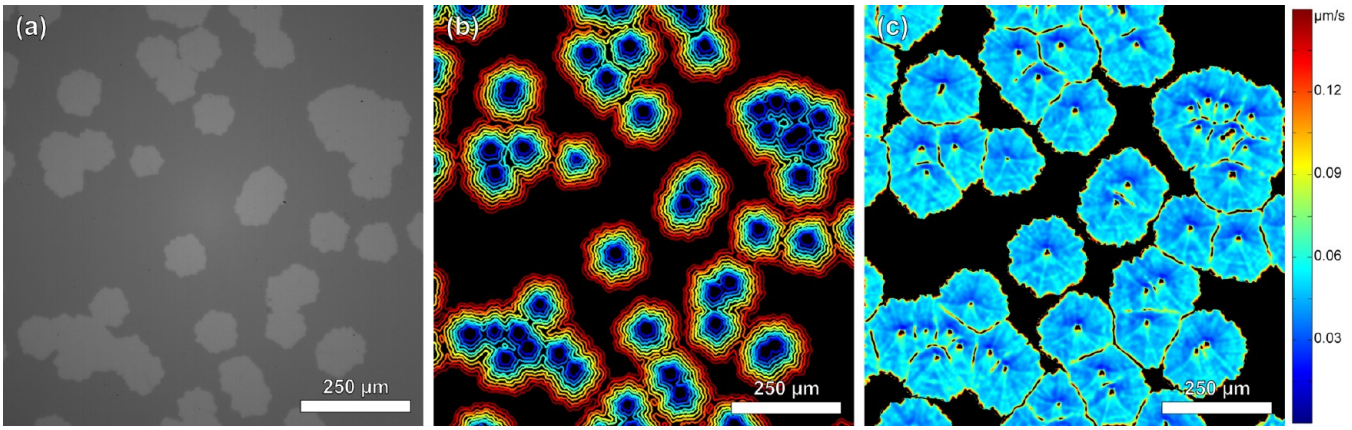

Figure 1. Image analysis performed to obtain the time mapping and crystal growth rate from a series of images obtained using optical microscopy. (a) Example image showing the as-recorded contrast between the amorphous (dark gray) and crystalline (light gray) phases as obtained after isothermal crystallization. (b) Using filtering and edge detection, the crystalline−amorphous interfaces are stored for all recorded images and combined into a single time mapping of the crystal growth. Each edge is given a value corresponding to the time it was recorded (for displaying purposes, the number of interfaces shown is strongly reduced with 160 s between successive growth fronts, and they are also thickened to more than one pixel wide). (c) Growth rate image as obtained by applying planar fits (typically, a circle with a radius of 8 pixels) to the data around each pixel in the time mapping, as shown in (b) (but then containing all data).

EXPERIMENTAL SECTION

Film Preparation. Samples investigated consist of 200 nm thin films with a Ge_6Sb_{94} or Ge_7Sb_{93} composition on a glass or polycarbonate substrate. The phase-change films were deposited on these substrates simultaneously using cosputtering with a Unaxis DVD Sprinter sputter coater. The deposition rate was 2.5 nm s^{-1}. All the phase-change films were directly capped with a 5 nm layer of ZnS-SiO_2 without breaking the vacuum. Both the polycarbonate and the glass substrates have a thickness of 1.3 mm.

Image Analysis. The crystal growth was observed using a high-speed optical camera (Photron 1024 PCI) with a zoom objective. The crystal growth rate was obtained quantitatively by analyzing typically 100−200 images obtained from the optical recordings. The crystalline areas in the image are determined by first subtracting the amorphous background and removing the remaining noise using binary open and close operations. The edges of the crystals are then found using Sobel edge detection. This is done for all recorded images. The edges (amorphous−crystalline interfaces) found in all separate images are combined into one time mapping, where the pixels pertaining to each edge receive a value corresponding to the recording time of the image it originated from. Fitting a plane (typically a circle with a radius of 8 pixels) to the nonzero data points around each pixel of the time mapping image gives us the derivative at each pixel, which is a direct measure of the inverse growth rate. By inversing each value, the crystal growth rate is obtained for each pixel. Note that the nonzero data points correspond to pixels that are on any of the growth fronts in the 100−200 images analyzed. The zero data points correspond to pixels that are in between successive growth fronts. These zero data points should not be included in the fitting procedure, because this would lead to errors in the growth rate values. In the growth rate image, it can also be verified whether the growth rate is constant in time or that a significant time dependence is present. A growth rate histogram is produced by combining all pixel values for the growth rate. The growth rate pertaining to the most prevalent value in the histogram is considered the relevant growth rate for the crystallization process. This procedure is also explained and applied in ref 13.

RESULTS AND DISCUSSION

Ge_6Sb_{94} and Ge_7Sb_{93} were selected as the phase-change materials to study, since they have a crystallization temperature around 100−140 °C,[14] well below the glass transition temperature of the polycarbonate substrate of 150 °C, but still they have a stable amorphous phase at room temperature. Moreover, Ge_6Sb_{94} and Ge_7Sb_{93} are fast-growth materials having a very low nucleation rate, resulting in large crystals, whose growth can be easily monitored optically. Isothermal crystallization experiments were performed in situ for both substrates. Crystal nucleation only occurred sufficiently long after the isothermal annealing temperature is reached, and therefore, the growth rates correspond to truly isothermal processes. From the recorded images, it was evident that the crystal growth rate at a certain temperature is independent of time.

The processing of an isothermal measurement at a temperature of 110 °C for a 200 nm thick Ge_6Sb_{94} film is shown in Figure 1. Figure 1a shows an unprocessed image as obtained from the optical recordings with the as-recorded optical contrast between the amorphous (gray) and crystalline (white) phases. Using filtering and edge detection, the crystalline−amorphous interfaces were detected for all the recorded images and combined in one time mapping; see Figure 1b. For visibility reasons, only a few interfaces are shown with their corresponding time in the color coding. From the time mapping, the growth rate image was obtained (see Figure 1c), where, apart from the singularities at the final edges and center of the crystals, a constant growth rate holds.

Isothermal measurements for the Ge_6Sb_{94} films were performed for the glass substrates for T = 90 °C up to T = 120 °C and for the polycarbonate substrates for T = 100 °C up to T = 135 °C with steps of 5 °C. The samples were heated to the desired temperature at a rate of 20 °C min^{-1}. The temperatures were stable within 0.2 °C. For each temperature, the crystal growth rate was determined and plotted in an Arrhenius plot (see Figure 2), where linear fits provided the activation energy for growth. For both substrates, similar activation energies are found: E_g = 1.68 ± 0.07 eV and E_g = 1.70 ± 0.07 eV for the polycarbonate and glass substrates, respectively. The intercepts are at $\ln(G)$ = 47.9 ± 1 and $\ln(G)$ = 50.5 ± 1, with G the growth rate in μm s^{-1}. This significant difference corresponds to a 6−7 times higher crystal growth rate on the glass substrate (compared to the polycarbonate substrate) for a given temperature in the temperature range discussed. To obtain a similar crystal growth rate on the

dx.doi.org/10.1021/cg3013848 | Cryst. Growth Des. 2013, 13, 220−225

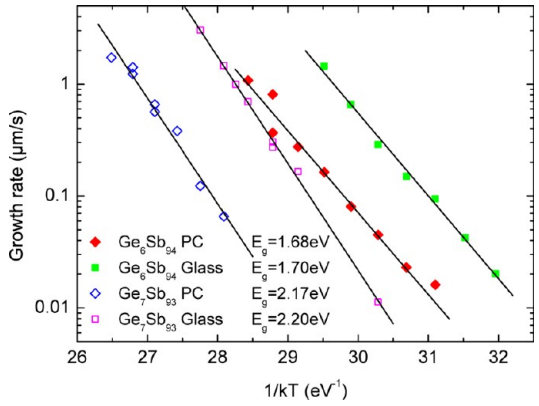

Figure 2. Crystal growth rate versus reciprocal temperature for Ge_6Sb_{94} (filled symbols) and Ge_7Sb_{93} (open symbols) phase-change films on glass (squares) and polycarbonate (diamonds) substrates. The activation energies for crystal growth found are similar for both substrates. A shift to significantly higher crystallization temperatures is found when using a polycarbonate substrate instead of a glass substrate.

polycarbonate substrate as that on the glass substrate, the annealing temperature has to be increased by ~15 °C. Similar results were found for the Ge_7Sb_{93} films between T = 110 °C and T = 160 °C. An activation energy for growth of E_g = 2.17 eV was determined for the polycarbonate substrate and E_g = 2.19 eV for the glass substrate. Similar to Ge_6Sb_{94}, there is a significant difference in the offset: $\ln(G)$ = 58.3 ± 1 for the polycarbonate substrate, and $\ln(G)$ = 62.1 ± 1 for the glass substrate. This corresponds for a given temperature to a 20−25 times higher crystal growth rate on the glass compared to the polycarbonate substrate.

This difference in offset (crystallization rate/temperature) is attributed to the difference in thermal expansion between the substrates and the phase-change film, resulting in large differences in thermal stresses. The thermal expansion coefficients for the different materials used are[15] α_{Sb} = 8.5 × 10^{-6} K^{-1} for antimony,[16] α_{PC} = 65 × 10^{-6} K^{-1} for polycarbonate, and α_{Gl} = 9.0 × 10^{-6} K^{-1} for glass. The in-plane biaxial stress in the phase-change film due to the difference in thermal expansion between the film and the substrate is estimated by

$$\sigma_{//} = \frac{E}{1-\nu}\Delta\alpha\Delta T \quad (1)$$

where E is the Young's modulus of the film (=54.4 GPa), ν is the Poisson's ratio of the film (=0.25), $\Delta\alpha$ is the difference in thermal expansion coefficient between the substrate and the film, and ΔT is the change in temperature. In this case, it is assumed that the strain in the film completely accounts for the difference in thermal expansion between the film and the substrate and that no significant stresses develop in the substrate. Moreover, isotropic elasticity is assumed. Within this framework, an in-plane tensile stress of $\sigma \approx 400$ MPa is expected in the PCM film on the polycarbonate substrate at 115 °C, whereas the stress is almost zero on the glass substrate.

The large difference in the growth rate for a given temperature depending on the substrate can be explained by this stress difference. As the amorphous film crystallizes, an in-plane tensile strain is introduced in the crystalline phase, as outlined above. During the crystallization process, enough (thermal) energy has to be provided to the system to overcome this tensile strain. Although the thermal stresses introduced in the film due to the mismatch with the substrate will relax, a significant elastic stress will remain. This stress, depending on its sign, will lower or increase the tensile strain that has to be overcome during crystallization and thus the energy needed for crystallization. This results, in agreement with the observations, in a significantly lower crystal growth rate at a given temperature for in-plane tensile stresses induced by the polycarbonate substrate in the PCM film compared to the fairly stress-free state in the case of the glass substrate. Direct proof that significant tensile stresses are present in the PCM films on polycarbonate substrates comes from the observations that, at high heating rates, cracks develop in the PCM film and, for the same heating rates, cracks were not observed in the PCM films on the glass substrates.

A more direct and controllable method to prove the large influence of stresses on the crystal growth is to use a four-point bending stage. By applying a certain deflection to the two inner

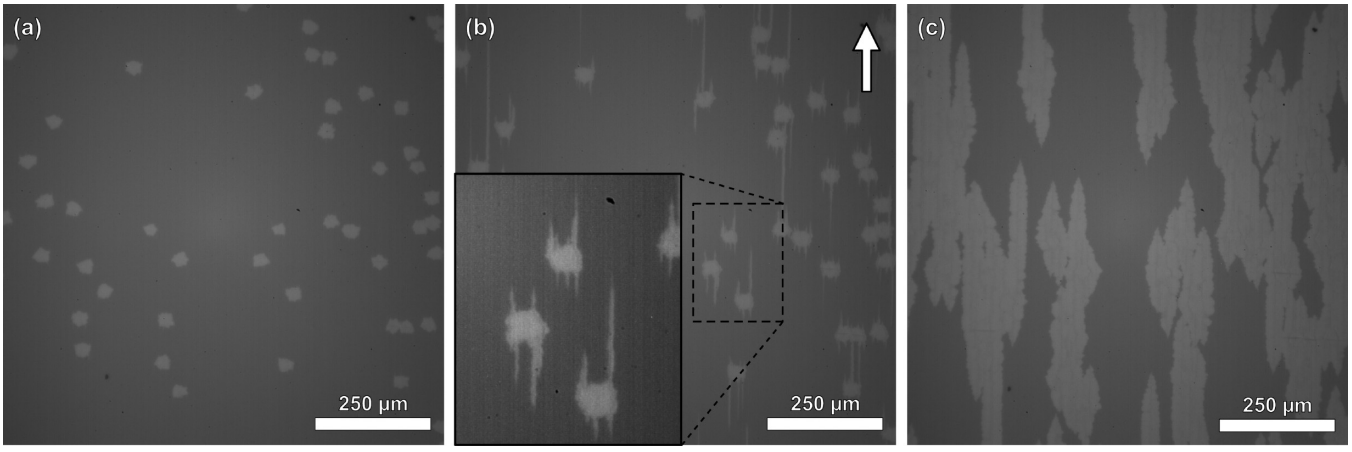

Figure 3. Crystal growth during a 70 MPa bending experiment at 115 °C in a Ge_6Sb_{94} film on a polycarbonate substrate as monitored optically. The arrow indicates the direction of the bending axis; the applied unidirectional in-plane compressive stress is perpendicular to the bending axis. (a) Isotropic crystal growth is visible before bending. (b) 75 s after the onset of bending the sample, crystal growth parallel to the bending axis is clearly visible. This one-dimensional growth occurs at a significantly higher speed than the isotropic growth before bending. (c) After 270 s, crystal growth has become nearly two-dimensional again, resulting in elongated crystals.

dx.doi.org/10.1021/cg3013848 | Cryst. Growth Des. 2013, 13, 220−225

beams of the four-point bending setup, a uniform moment is created in between these two inner beams. For our work, only the region in between these two inner beams is relevant. Next, it is important to note that we have a (200 nm) thin film on a (1.3 mm) thick substrate. Therefore, the gradient in stress over the thickness of the whole sample during bending, which ranges from compressive on one side to tensile on the other side of the sample, can be neglected for the thin film. This results in a uniform unidirectional stress being applied in the thin film perpendicular to the bending axis. By measuring the deflection at the center relative to the two inner beams, the curvature of the substrate is measured from which the stress in the film can be calculated using standard solid mechanics. Different stresses ranging between 10 and 120 MPa were applied by using different deflection distances. We verified that, in all cases, the film stays attached to the substrate and thus follows the elastic strains of the substrate. In the bending experiments, we used samples with a polycarbonate substrate. We could only use compressive stresses in the PCM films, because when we tried tensile stresses, the PCM films showed cracks, which prevent any relevant analysis of the influence of tensile stresses on the growth rate.

The whole stage, including the sample with a Ge_6Sb_{94} film, was heated to 115 °C before the bending was performed to prevent relaxation of the applied stresses during the heating and annealing process. This turned out to be crucial. After small, but optically clearly visible, crystals had formed in the film with an average diameter of 30 μm, the compressive bending stress was applied. As soon as the stress was applied, it was clearly visible that the crystal growth became severely anisotropic; see Figure 3. For small stresses (<50 MPa), the crystals became diamond-shaped, elongated along the bending axis. For larger stress, the crystals initially only grow in one direction at a much higher growth rate than before bending (Figure 3b), resulting in long thin crystalline needles parallel to the bending axis originating from the isotropic grown crystals already present. After the initial fast one-directional growth, the growth rate decreased and the crystal growth continued in all directions (Figure 3c). The same effects were observed in Ge_7Sb_{93} films.

In agreement with the isothermal experiments, where in-plane thermal tensile stresses increased the crystallization temperature, we now see during the bending experiments a strong increase in crystal growth rate at a certain temperature, that is, a decrease in crystallization temperature when compressive stresses are applied.

For understanding the effect on crystallization of applying a 1D compressive stress to a thin film, the analogy with applying a 1D tensile stress on crack opening and crack growth in a thin film is very instrumental. Figure 4 shows a schematic representation of this clear analogy. Under tensile stress, the original circular crack grows in a direction perpendicular to the applied stress in order to relax the residual stress in the system. Similarly, the original circular crystal grows perpendicular to the applied compressive stress in order to relax the residual stress in the system for the general case that the crystalline phase has a higher density than the amorphous phase.

The crystal growth during the bending experiment was observed and analyzed as described above. However, a drawback of the planar fitting used is that it gives a large error at the edges; a sharp change in growing direction cannot be properly fitted with a plane surface. Therefore, because of the shape of the long thin crystals, line profiles were taken along the length or width of the crystals, as shown in Figure 5.

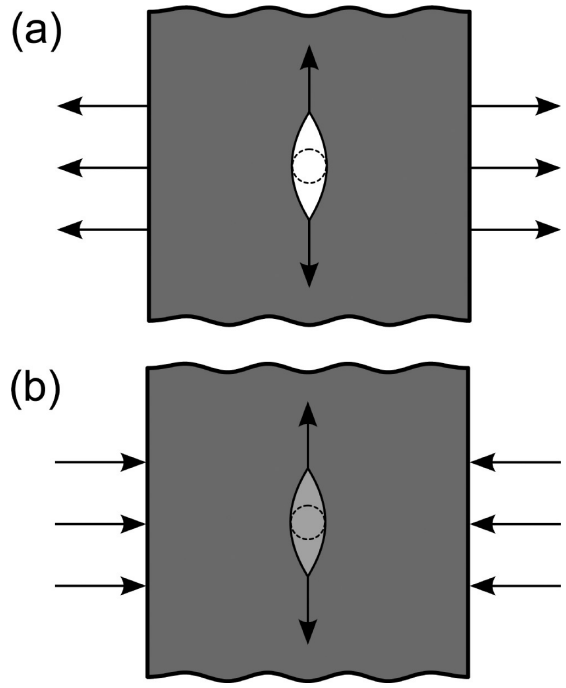

Figure 4. Analogy between (a) crack growth in a plate under a one-dimensional (1D) tensile stress and (b) crystallization under a 1D compressive stress.

A linear fit was applied to these line profiles to obtain the crystal growth rates.

Figure 5a,b shows the time mappings of the bending experiments for an applied compressive bending stress of 40 and 70 MPa. For 70 MPa, we can clearly observe that there is a strong preference for unidirectional growth; the crystals are elongated in the direction parallel to the bending axis. Line profiles taken from the time mappings along the width of the crystals are shown in Figure 5c,d. For both 40 and 70 MPa, we obtain a crystal growth rate $v = 0.11 \pm 0.01$ μm s^{-1} parallel to the bending axis, which corresponds to the crystal growth rate at 115 °C for a nonbended sample; that is, the applied bending does not change the growth rate perpendicular to the bending axis. For the growth parallel to the bending axis, we do see a difference between bended and nonbended samples. When a stress of 40 MPa is applied, we initially observe a growth rate of 0.4 μm s^{-1}. After 70 s, the crystal growth rate decreases relatively abruptly to 0.15 μm s^{-1}. This is still higher than the growth rate found perpendicular to the bending axis and the nonbended growth rate. Applying a bending stress of 70 MPa leads to an initial crystal growth rate of 6.7 μm s^{-1}, which is 60 times higher than that for the nonbended case. After 20 s, the crystal growth rate decreases relatively abruptly to 0.26 μm s^{-1}, which is still more than twice the unstressed crystal growth rate.

A direct cause for the observed abrupt transition to a lower growth rate is the relaxation of the applied compressive stress, reducing the driving force for accelerated unidirectional crystallization. This relaxation is attributed to crystallization of the phase-change material and to plastic deformation in the substrate as the sample is at an elevated temperature. We have proof for plastic deformation in the polycarbonate substrate, because, when the sample is removed from the bending stage after the bending experiment at elevated temperature, the sample only partly flexes back and thus partly remains bended. Moreover, there is experimental data[17] that stress relaxation in

dx.doi.org/10.1021/cg3013848 | Cryst. Growth Des. 2013, 13, 220−225

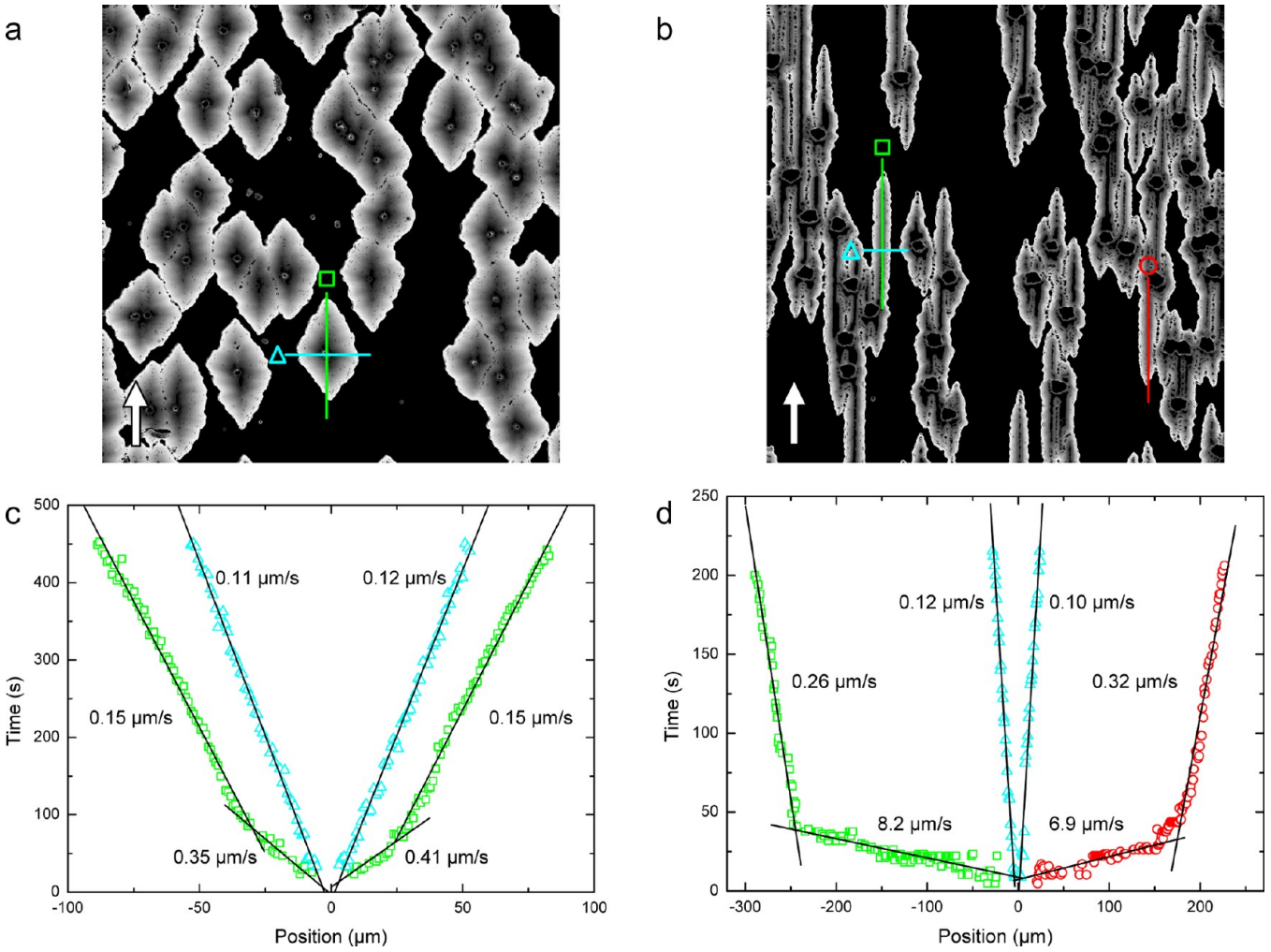

Figure 5. (a, b) Time mappings with the white arrow indicating the bending axis. (c, d) Line profiles taken along the corresponding lines shown in (a) and (b) for a compressive bending stress of (a, c) 40 MPa and (b, d) 70 MPa. After an initially increased crystal growth rate parallel to the bending direction (squares and circles), the crystal growth rate decreases strongly but remains significantly higher than the unstressed growth perpendicular to the bending axis (triangles).

PCMs at the applied temperatures takes considerably longer (several thousand seconds) than the times of our experiments (not more than a few hundred seconds). This explains why the growth rate in the PCM film, after the initial abrupt drop in growth rate due to relaxation of the substrate, is still higher at a given temperature than that for the stress-free case, because stress relaxation in the amorphous phase of the PCM is not completed yet. We cannot measure these long times needed for full stress relaxation, that is, when the growth rate in all directions becomes the same, because the film is already fully crystallized much earlier.

We have additional evidence that the effect of bending stress on the increase in growth rate is highly nonlinear; see Figure 6. After bending stresses are applied, crystals in the phase-change films develop into elongated shapes with their long axis parallel to the bending axis. These shapes, therefore, provide a measure for the increase in crystal growth rate due to the applied stresses. By measuring the aspect ratio, that is, the length divided by the width of the crystals at a fixed time after the bending was applied, a lower bound for this increase (multiplication factor) in growth rate due to the applied stresses was obtained. It is a lower bound because the crystals are measured at a time when the growth parallel to the bending

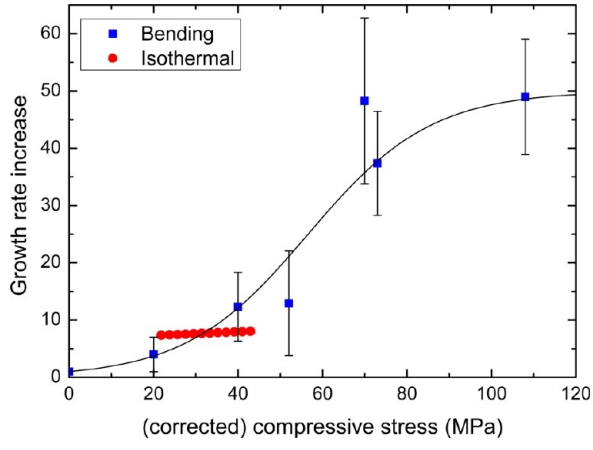

Figure 6. Growth rate increase (multiplication factor) for bending (blue squares) and isothermal (red circles) experiments performed on Ge_6Sb_{94} films as a function of applied compressive stress, where, for the isothermal measurements, the calculated stress has been reduced by 90% to match the data with the results from the bending experiments. For higher compressive bending stresses, the growth rate increase levels off. The solid black line is a guide to the eye.

dx.doi.org/10.1021/cg3013848 | *Cryst. Growth Des.* 2013, 13, 220−225

axis has lost (due to stress relaxation already in an earlier stage) its initial fast rate. Figure 6 shows that the increase in growth rate is highly nonlinear: up to 40−50 MPa, the increase is modest; then, in the regime from 40 to 70 MPa, the increase becomes very pronounced. However, this increase then levels off at stresses beyond 100 MPa, probably because increasing stress beyond this value only causes additional plastic deformation and not an increasing elastic stress required to alter the growth rate. The relatively large error bars in Figure 6 are a result of the large spread in aspect ratios found in the experimental images, and this large spread also reflects the different times crystals with accelerated unidirectional growth started to grow (nucleated) out of the earlier isotropically grown crystals. Crystals that start to grow immediately after applying the bending stress have the highest aspect ratio, and crystals that start to grow later experience a condition with more stress relaxation, and will thus have a lower aspect ratio.

The results in Figures 5 and 6 demonstrate that compressive stresses in the range of 70−120 MPa accelerate the crystal growth at least 40 times. From the isothermal experiments, where the stress difference in the film due to the different substrates was calculated to be in the order of 400 MPa, we see a 6-fold increase in growth rate for the Ge_6Sb_{94} films on the glass compared to the polycarbonate substrates. For the bending experiments, we find the same increase in growth rate already at a compressive bending stress of only 20−40 MPa. If we assume that the measurement of the growth rate increase during the bending experiment, as shown in Figure 6, matches the corresponding growth rate increase found from the isothermal experiments, we find that the calculated stresses from the isothermal experiments have to be reduced by 90% to match the data obtained from bending experiments. This would mean that the thermal stresses induced in the phase-change film due to the difference in thermal expansion coefficient between substrate and film are relaxed by about 90% during the heating process. This amount of relaxation matches well with the result (i.e., 91% relaxation) found in ref 8.

CONCLUSIONS

Using optical microscopy, we have demonstrated that stresses in phase-change films have a pronounced effect on the crystal growth rate. For Ge_6Sb_{94} and Ge_7Sb_{93} phase-change films, a large increase in crystallization temperature was found when using a polycarbonate substrate instead of a glass substrate. This increase is attributed to the tensile thermal stress induced in the phase-change film due to a difference in thermal expansion coefficient between the film and the polycarbonate substrate. We also demonstrated that applying a compressive bending stress of only 70 MPa already leads to a 60-fold faster crystal growth parallel to the bending axis, that is, perpendicular to the applied compressive stress. This is a direct proof that modest stresses can have large consequences for the amorphous phase stability and for the crystal growth rates, and these stresses are thus highly relevant for memories based on PCM.

AUTHOR INFORMATION

Corresponding Author

*E-mail: gerteising@gmail.com (G.E.), b.j.kooi@rug.nl (B.J.K.).

Notes

The authors declare no competing financial interest.

ACKNOWLEDGMENTS

This research was carried out under project number M62.7.08SDMP03 in the framework of the Industrial Partnership Program on Size Dependent Material Properties of the Materials innovation institute M2i (www.m2i.nl) and the Foundation of Fundamental Research on Matter (FOM) (www.fom.nl), which is part of The Netherlands Organisation for Scientific Research (www.nwo.nl). We also want to thank Prof. Patrick Onck for fruitful discussions.

REFERENCES

(1) Wuttig, M.; Yamada, N. *Nat. Mater.* **2007**, *6*, 824−832.
(2) Raoux, S. *Annu. Rev. Mater. Res.* **2009**, *39*, 25−48.
(3) Lencer, D.; Salinga, M.; Wuttig, M. *Adv. Mater.* **2011**, *23*, 2030−2058.
(4) Burr, G. W.; Breitwisch, M. J.; Franceschini, M.; Garetto, D.; Gopalakrishnan, K.; Jackson, B.; Kurdi, B.; Lam, C.; Lastras, L. A.; Padilla, A.; Rajendran, B.; Raoux, S.; Shenoy, R. S. *J. Vac. Sci. Technol., B* **2010**, *28*, 223−261.
(5) Schneider, M. N.; Urban, P.; Leineweber, A.; Döblinger, M.; Oeckler, O. *Phys. Rev. B* **2010**, *81*, 184102.
(6) (a) Braga, S.; Cabrini, A.; Torelli, G. *Appl. Phys. Lett.* **2009**, *94*, 092112. (b) Mitra, M.; Jung, Y.; Gianola, D. S.; Agarwal, R. *Appl. Phys. Lett.* **2010**, *96*, 222111.
(7) Njoroge, W. K.; Woltgens, H.-W.; Wuttig, M. *J. Vac. Sci. Technol., A* **2002**, *20*, 230−233.
(8) Pedersen, T. P. L.; Kalb, J.; Njoroge, W. K.; Wamwangi, D.; Wuttig, M.; Spaepen, F. *Appl. Phys. Lett.* **2001**, *79*, 3597−3599.
(9) Xu, M.; Meng, Y.; Cheng, Y. Q.; Sheng, H. W.; Han, X. D.; Ma, E. *J. Appl. Phys.* **2010**, *108*, 083519.
(10) Simpson, R. E.; Krbal, M.; Fons, P.; Kolobov, A. V.; Tominaga, J.; Uruga, T.; Tanida, H. *Nano Lett.* **2010**, *10*, 414−419.
(11) Park, I.-M.; Jung, J.-K.; Ryu, S.-O.; Choi, K.-J.; Yu, B.-G.; Park, Y.-B.; Han, S. M.; Joo, Y.-C. *Thin Solid Films* **2008**, *517*, 848−852.
(12) Guo, Q.; Li, M.; Li, Y.; Shi, L.; Chong, T. C.; Kalb, J. A.; Thompson, C. V. *Appl. Phys. Lett.* **2008**, *93*, 221907.
(13) Oosthoek, J. L. M.; Kooi, B. J.; De Hosson, J. T. M.; Wolters, R. A. M.; Gravesteijn, D. J.; Attenborough, K. *Microsc. Microanal.* **2010**, *16*, 291−299.
(14) Raoux, S.; Cabral, C.; Krusin-Elbaum, L.; Jordan-Sweet, J. L.; Virwani, K.; Hitzbleck, M.; Salinga, M.; Madan, A.; Pinto, T. L. *J. Appl. Phys.* **2009**, *105*, 064918.
(15) Martienssen, W., Warlimont, H., Eds. *Springer Handbook of Condensed Matter and Materials Data*; Springer: Heidelberg, 2005.
(16) We use α_{Sb} as the thermal expansion coefficient for the phase-change films since data could not be found for the alloys used and their composition is relatively close to pure Sb.
(17) Park, I.-M.; Cho, J.-Y.; Yang, T.-Y.; Park, E. S.; Joo, Y.-C. *Jpn. J. Appl. Phys.* **2011**, *50*, 061201.